STM JOURNALS

International Journal of
Molecular Biotechnological Research

Volume 2, Issue 1, 2024
January–June
DOI (Journal): 10.37591/IJMBR

https://journals.stmjournals.com/ijmbr

Research IJMBR

Integrating Network Pharmacology and Molecular Docking to Investigate *Boerhavia diffusa* for Pancreatic Cancer Treatment

Gouri Anil*

Abstract

Objective: *In this study, network pharmacology was applied to determine the therapeutic effects of the bioactive compounds of Boerhavia diffusa. Network pharmacology can unearth the underlying mechanisms between drugs and the disease targets and aids in the discovery of novel medications for complex conditions such as cancer.* ***Methods:*** *To predict the molecular mechanisms of action of Boerhavia diffusa in the treatment of was screened using the GeneCards database. The Venn diagram was used to identify the intersecting targets of Boerhavia diffusa and Alzheimer's disease. The obtained target information was entered into the STRING database to construct a protein-protein interaction network. Database for Annotation, Visualization, and Integrated Discovery (DAVID) database was used to perform the GO and KEGG Pathway Enrichment analysis. Cytoscape Software was used to construct the networks, and the key targets were identified. The binding affinity of the bioactive compounds of Boerhavia diffusa with the target proteins was analyzed. PyRx, an online tool was used to perform molecular docking. It was performed using protein structures from the Protein Data Bank (PDB) Database and PubChem. BIOVIA Discovery Studio software was used to analyze the protein structure.* ***Result:*** *Upon performing molecular docking, the proteins AKT1, epidermal growth factor receptor (EGFR), and STAT3 have the best binding affinities with the bioactive compounds of Boerhavia diffusa.* ***Conclusion:*** *According to the results, the phytocompounds have potential therapeutic effects which provide insight into the theoretical basis for the investigation of the pharmacological mechanism of Boerhavia diffusa. Alzheimer's disease using network pharmacology, the phytocompounds were obtained from the IMPPAT database. Target information for the phytocompounds and Alzheimer's disease.*

Keywords: Pancreatic cancer, *Boerhavia diffusa*, AKT1, EGFR, STAT3, Network Pharmacology, molecular docking

INTRODUCTION

Pancreatic cancer (PC) causes more than a quarter of the deaths annually and is among the tumors with the worst survival rates [1]. Early diagnosis is difficult because most patients do not display conspicuous indications during development and progression, which results in a metastatic stage involving highly invasive cancer cells [2]. Surgical resection in the form of resectable PC, handover resectable PC, unresectable PC, or distant metastasis is the only treatment option that can significantly prolong survival [3]. It has been demonstrated that resection surgery is more likely to succeed if the patient has been subjected to full-dose chemotherapy before surgery [4]. Previous research has demonstrated that adjuvant chemotherapy can be used to improve the therapeutic effects of surgery [5]. Other treatment options, such as radiation therapy [6] and targeted therapy based on biomarker-targeting antibodies

***Author for Correspondence**
Gouri Anil
E-mail: gourianil20@gmail.com

Student, Department of Biotechnolgy,People's Education Society University, Bangalore, Karnataka, India

Received Date: April 04, 2024
Accepted Date: April 16, 2024
Published Date: August 08, 2024

Citation: Gouri Anil. Integrating Network Pharmacology and Molecular Docking to Investigate *Boerhavia diffusa* for Pancreatic Cancer Treatment. International Journal of Molecular Biotechnological and Research. 2024; 2(1): 29–49p.

[7], along with palliative therapy [8, 9], have been incorporated to increase the survival rates of patients with PC. However, the 5-year survival rate is only 11%, as the tumor microenvironment is associated with primary and acquired resistance to therapy. [10, 11]. Furthermore, chemotherapy often has adverse effects on patients, including fatigue, nausea, and chemotherapy-associated oxidative stress [12]. Therefore, there is an urgent need to develop novel medications that are effective in treating PC. Table 1 presents the full forms of all the abbreviations used in this study.

Ayurvedic medicine is a traditional system of medicine that provides information on nature-based medicinal remedies that are heavily based on the relationship between the human body and elements of nature [13]. Several medicinal plants and herbs such as Ashwagandha [14], Tulsi [15], Shunti [16], and Guduchi [17] have been used for centuries to treat most types of cancers in Asian countries, including India [18].

Boerhavia diffusa (BD) is one such plant widely known for its renowned medicinal properties such as antiaging, disease prevention, and improved cognitive function, along with hepatoprotection and immunomodulation [19]. The plant possesses anti-cancer and anti-inflammatory properties from glycolic and lignan glycosides, flavonoid glycosides, isoflavonoids, steroids, and alkaloids, which are derived from various classes of secondary metabolites [20–22].

Ayurveda involves synergistic treatment that uses the multi-component nature of herbs to create formulations that increase efficacy [23]. Network pharmacology has proven to be a valuable tool for understanding the interactions of drugs with multiple targets by integrating systems biology, bioinformatics, and polypharmacology [24]. Using computational power, the molecular interactions between genes and protein targets related to diseases can be cataloged [25, 26], and new drug leads and targets can be discovered for different diseases [27]. The "one-drug, one-target" approach has proved to be useful but has its own set of limitations. Conditions such as cancer are the outcomes of several aberrant pathways, genes, and proteins, and cannot be treated effectively with treatment targeting one pathway, gene, or protein. Network pharmacology can provide better outcomes as it involves pharmacological action on several pathways [28].

METHODOLOGY

Data Preparation

Identification of Active Compounds of BD

Compounds found in BD were obtained from the Indian Medicinal Plants, Phytochemistry, and Therapeutics (IMPPAT) database (https://cb.imsc.res.in/imppat) [29].

The Screening of Bioactive Compounds in BD

Several ADME-related parameters can be employed, including oral bioavailability (OB), Drug Likeliness (QED), Number of Lipinski's rule violations, and gastrointestinal absorption, to assess the compounds of their ability as drug candidates [30]. SwissADME was used to evaluate them (http://www.swissadme.ch/index.php) [31] and ADMETLab 2.0 (https://admetmesh.scbdd.com/service/screening/index) [32] that are online databases that provide information on the ADME properties on the compounds.

Target Genes Prediction of BD Bioactive Compounds

The databases used to collect the potential targets of the phytochemicals were the SwissTargetPrediction Web server (http://www.swisstargetprediction.ch/) [33] and Similarity Ensemble Approach Search Server (SEA) (https://sea.bkslab.org/) [34].

Prediction of PC Target Genes

The data for the targets associated with PC were obtained from GeneCards (https://www.genecards.org/) [35], with the identifier set as "Pancreatic cancer" and the relevance score was set to greater than 30.

Table 1. List of abbreviations

Abbreviation	Full Form
AKT1	RAC-alpha serine/threonine-protein kinase
ADMET	Absorption, Distribution, Metabolism, Excretion and Toxicity
BBB	Blood-Brain Barrier
BD	*Boerhavia diffusa*
CCT	Compound-Compound Target
CTP	Compound-Target-Pathway
EGFR	Epidermal growth factor receptor
ESR1	Estrogen Receptor Alpha Gene
GO	Gene Ontology
OB	Oral Bioavailability
KEGG	Kyoto Encyclopedia of Genes and Genomes
PPI	Protein-Protein Interaction
PC	Pancreatic cancer
QED	Drug Likeliness
STAT3	Signal transducer and activator of transcription 3
TP	Target Pathway

Construction of Venn Diagram

Venny 2.0, was used to identify common targets between the predicted targets of the bioactive compounds of BD and the PC target genes (https://bioinfogp.cnb.csic.es/tools/venny/) [36].

Pathway Enrichment Analysis

The Database for Annotation, Visualization, and Integrated Discovery (DAVID) (https://david.ncifcrf.gov/tools.jsp) [37] was used to perform gene enrichment analysis, with the p-value cutoff set to less than or equal to 0.05. The pathways were sorted based on count (largest to smallest) and a bubble plot was constructed with the top 20 results. Bubble plots of the enrichment results were constructed using the Science and Research Online Plot (SRPLOT) (https://www.bioinformatics.com.cn/en) [38].

Network Construction

Networks represent interactions among herbal formulae, genes, and diseases and can be constructed using Cytoscape (version 3.1.0) (https://cytoscape.org/) [39]. CytoHubba [40] plugin was used to construct the subnetworks. The Compound-Compound Target Network was obtained by connecting the compounds with their corresponding targets.

Protein-protein interaction (PPI) data were obtained from the Search Tool for the Retrieval of Interacting Genes/Proteins (STRING) database (https://string-db.org/) [41]. Within STRING, PPIs are categorized based on data scores indicating their confidence levels (low: <0.4; medium: 0.4-0.7; high: >0.7). The species was restricted to “Homo sapiens,” the query was set only to PC-related targets, and interactions with confidence scores greater than 0.4 was considered.

The target-pathway network was constructed using the top 20 enriched genes identified through KEGG Pathway enrichment analysis, and this network was assembled using Cytoscape Software (Version 3.1.0) [39].

The top 20 enriched genes identified through KEGG Pathway enrichment analysis were used to construct the target-pathway network and were assembled using Cytoscape Software (Version 3.10)

[39]. The compound-target-pathway network was constructed by employing the "Merge" feature in Cytoscape Software (Version 3.1.0) [39], the compound-target-pathway network was constructed.

Molecular Docking Study

Protein Retrieval and Purification

Based on the analysis of the subnetworks, three proteins were chosen for the docking process based on analysis of the subnetworks. Proteins were retrieved from the Research Collaboratory for Structural Bioinformatics (RCSB) Protein Data Bank (PDB) database (https://www.rcsb.org/) [42]. The Water molecules and bound ligands were removed Using BIOVIA Discovery Studio Visualizer [43]. Using the AMBR force field, energy minimization was performed after the hydrogen atoms were removed using the USF CHIMERA Software (https://www.cgl.ucsf.edu/chimera/) [44].

Secondary Structural Analysis

Secondary structure analysis was performed using PDBsum [45] (http://www.ebi.ac.uk/pdbsum.). Ramachandran plots and predicted secondary structures were analyzed to understand the structure of the protein.

Molecular Docking

Molecular docking between the ligands and proteins was performed using PyRx software [46]. The BIOVIA Discovery Studio Visualizer provides the opportunity to view the interactions in the form of 2D diagrams [43], and the protein-ligand complex can be viewed using PyMol Software [47]. The binding pockets of the proteins were downloaded using PrankWeb (https://prankweb.cz/) [48] and compared to the interactions visualized in 2D diagrams to understand the ligand-protein complex.

RESULTS

Collection of Bioactive Compounds of BD

64 phytocompounds of BD were obtained from IMPPAT out of which 56 were unique.

Screening of Bioactive Compounds in BD

ADME-related parameters, including OB ≥30%, QED ≥0.18, high GI absorption, and 0 Lipinski's rule violations, were used to screen 56 compounds collected from the IMPPAT database. Nineteen compounds passed the ADME screening and are presented in Table 2.

Target Genes Identification for BD Bioactive Substances

When the search was restricted to "Homo sapiens" and a probability greater than zero, 402 targets were found from the SEA search server [44] and the SwissTargetPrediction database [43].

Prediction of PC Target Genes

A total of 4368 PC-related targets with a relevancy score > 30 were found when the search term "pancreatic cancer" was used in GeneCards [45].

Construction of Venn Diagram

A Venn diagram was constructed, which represented 62 intersecting targets between 402 putative targets of the compounds and 560 PC-related targets. This is illustrated in Figure 1.

Pathway Enrichment Analysis Using GO and KEGG

GO and KEGG enrichment studies were carried out on 62 targets to uncover biological activities and metabolic pathways. The GO and KEGG Pathway Enrichment analysis findings, shown in Figure 2, are graphically depicted using bubble diagrams after filtering with a p-value <0.05. A total of 438 biological processes (BP), 53 cellular components (CC), and 96 molecular functions (MF) were identified using GO analysis. The primary processes regulated by BP targets include protein autophosphorylation, positive regulation of cell proliferation, negative control of apoptosis, and positive regulation of the ERK1 and ERK2 cascades.

Table 2. Lists the ADME characteristics of the BD bioactive substances that cleared the screening.

Compounds	GI Absorption (High)	OB >= 30%	QED >=0.18	Lipinski's Rules
Ascorbic acid	High	0.56	0.412	Accepted
Oxalic acid	High	0.85	0.38	Accepted
boeravinone D	High	0.55	0.624	Accepted
boeravinone E	High	0.55	0.468	Accepted
boeravinone C	High	0.55	0.722	Accepted
Liriodenine	High	0.55	0.494	Accepted
Eupalitin	High	0.55	0.677	Accepted
boeravinone B	High	0.55	0.552	Accepted
boeravinone A	High	0.55	0.714	Accepted
boeravinone F	High	0.55	0.258	Accepted
Diffusarotenoid	High	0.55	0.633	Accepted
3,3′,5-trihydroxy-7-methoxyflavone	High	0.55	0.672	Accepted
4′,7-dihydroxy-3′-methylflavone	High	0.55	0.711	Accepted
Palmitoleic acid	High	0.85	0.356	Accepted
Myristic acid	High	0.85	0.488	Accepted
Repenone	High	0.55	0.435	Accepted
Xanthone	High	0.55	0.517	Accepted
Oxalic acid	High	0.85	0.38	Accepted
Lunamarine	High	0.55	0.73	Accepted
L-Rhamnose	High	0.55	0.326	Accepted

Targets in CC mostly involve the cytoplasm, neoplasm, plasma membrane, cytosol, and the nucleus. They are also involved in receptor complex formation. As shown in Figure 2(c), the primary objectives of MF are protein-binding, enzyme binding, ATP binding, protein kinase activity, identical protein activity, DNA-binding, and protein homodimerization activity. Following KEGG Pathway analysis, 135 pathways were identified, with the majority of the targets being involved in pathways related to cancer, including the P13K-Akt, MAPK, microRNA, and proteoglycan pathways; pathways related to Ras and Rap1; and pathways related to breast, gastric, prostate, and pancreatic cancers. According to GO and KEGG Pathway Enrichment analyses, BD may be involved in PC therapy through the aforementioned pathways, 40 of which are potential targets in cancer. The top 20 words and routes were chosen to create the bubble plots shown in Figure 2 (d) after the terms and pathways were sorted by count (largest to smallest).

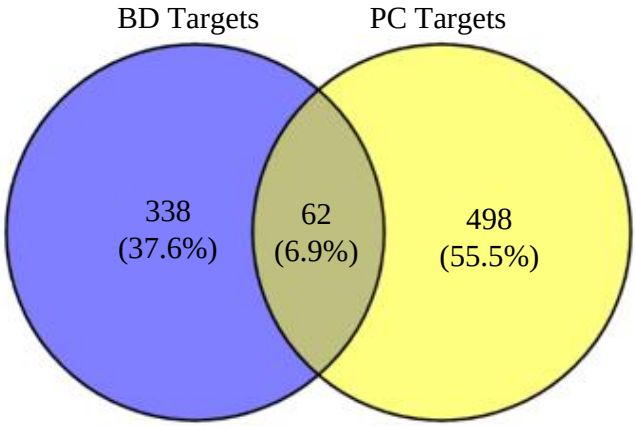

Figure 1. Venn diagram representing the intersecting targets.

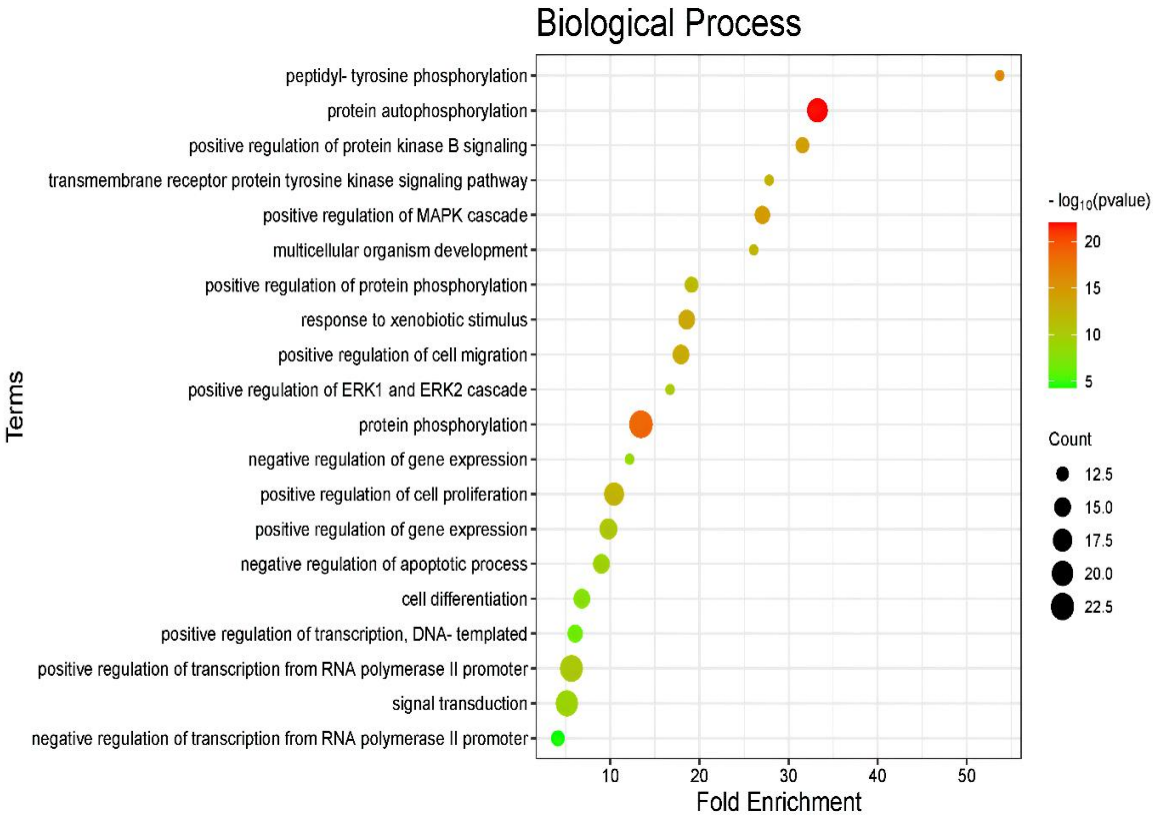

Figure 2. (a). Biological process GO enrichment analysis.

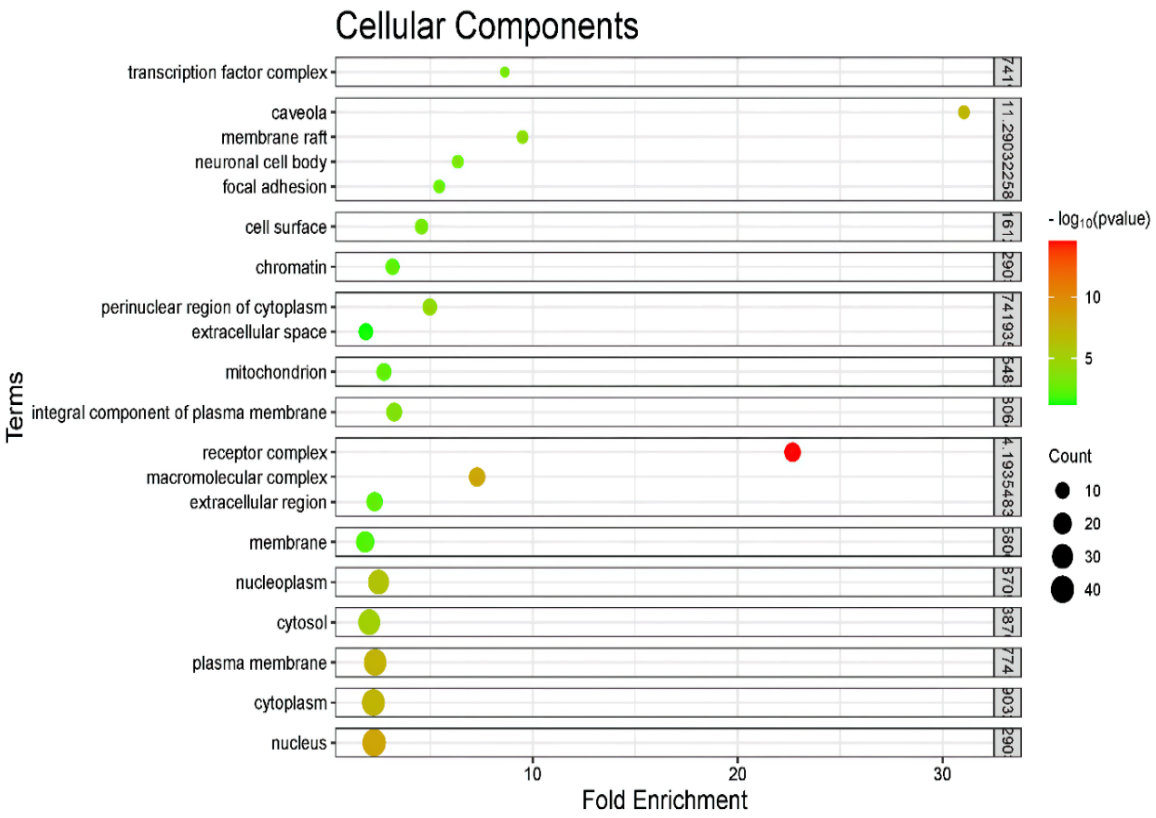

Figure 2. (b). GO enrichment analysis of the cellular components.

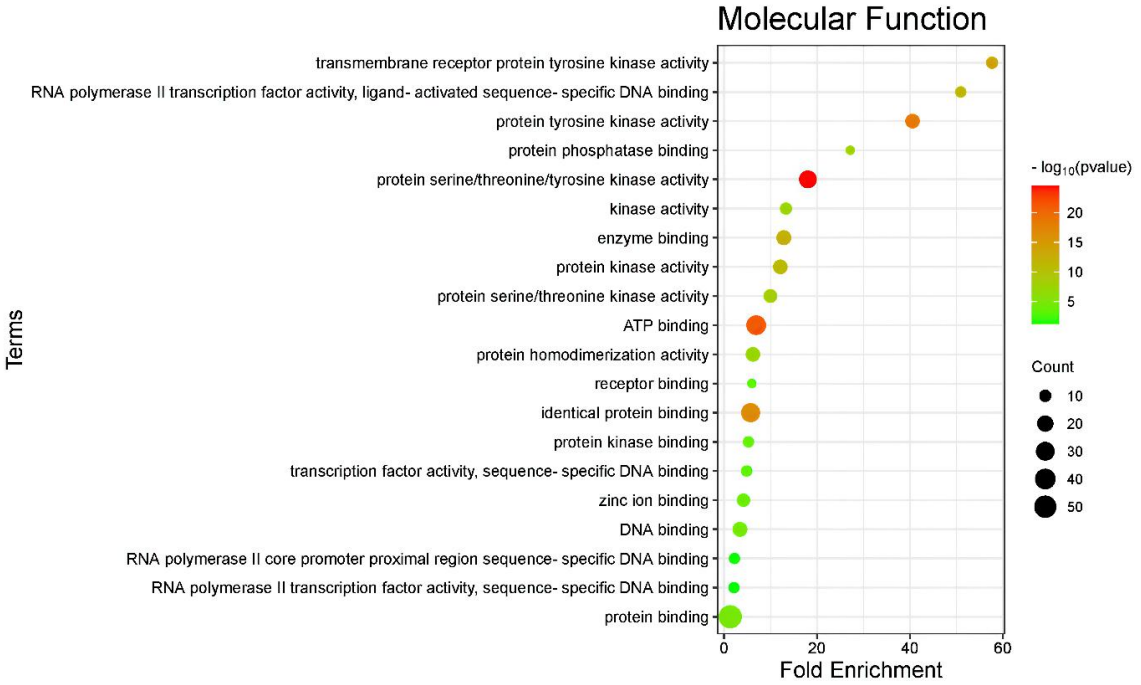

Figure 2. (c). Molecular Function Enrichment Analysis using GO.

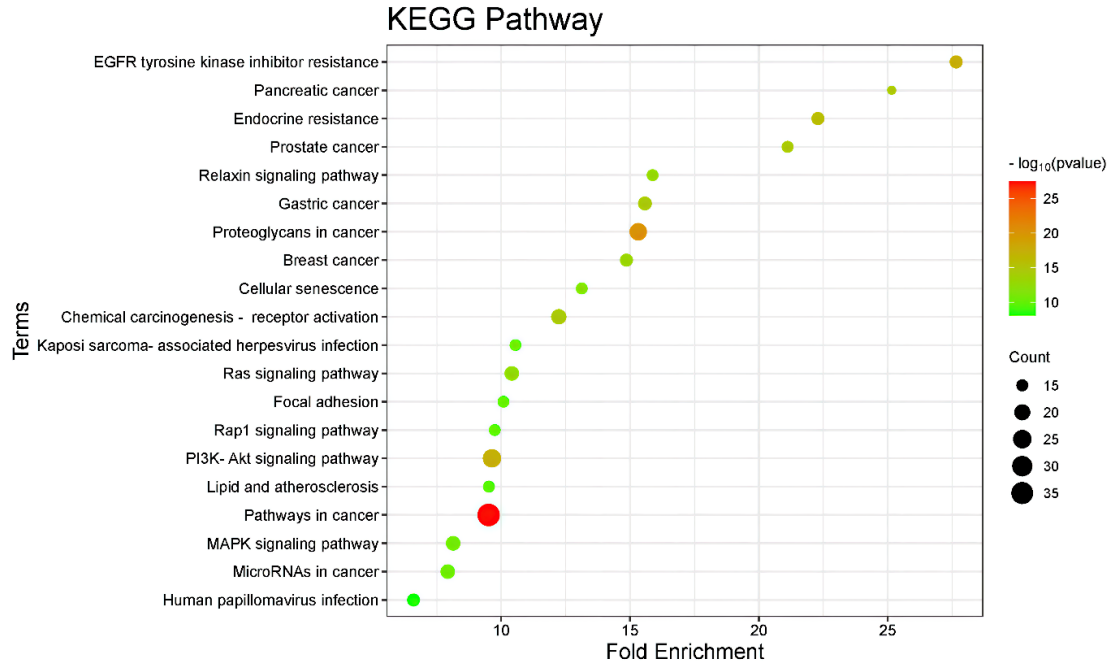

Figure 2. (d). Analysis of KEGG Pathway Enrichment.

The findings of the enrichment study indicated that the biological mechanisms and cellular constituents associated with BD targets vary and participate in several metabolic pathways, thus validating its multi-pathway attributes.

Network Construction

Compound-Compound Target Network

The compound-target-pathway has also been constructed [~~51~~49]. With 418 nodes and 823 edges, the compound target shown in Figure 3 had a network density of 0.009 and a network diameter of 7. The

targets were represented by edges, whereas the compounds were represented by nodes. It was found that a molecule involves many genes and that some genes overlap with other compounds.

Based on "degree," the sub-network was built using the CytoHubba Plugin [~~52~~50] to determine which Hub compounds had the most interactions. Five Hub molecules with a degree of 100 were identified by sub-network analysis: eupalitin, liriodenine, 4,7-dihydroxy-3′-methylflavone, 3,3′,5-trihydroxy-7-methoxyflavone, and lunamarine. This suggests that these substances are the most important in BD. Figure 4 shows the sub-network corresponding to the top 10 important chemicals. Table 3 displays the 2D structures of the Hub compounds obtained from the PubChem Database [~~76~~51].

The interactions between the BD compounds and their targets are illustrated by blue triangles, representing the active compounds, and green ellipses, representing the targets.

Triangles represent the target proteins and the color gradient from red to yellow represents the highest to lowest degree.

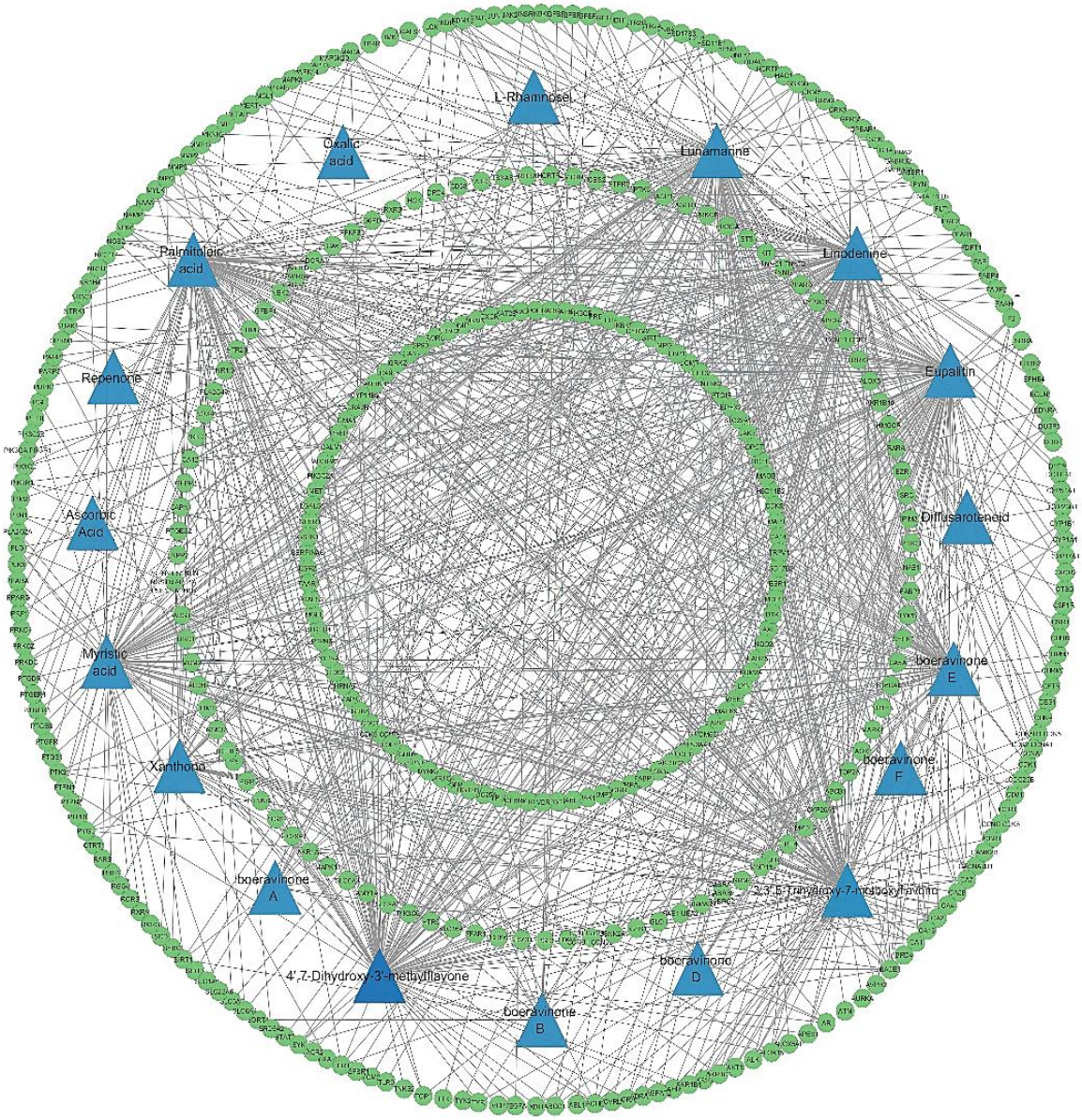

Figure 3. Compound-Compound Target Network.

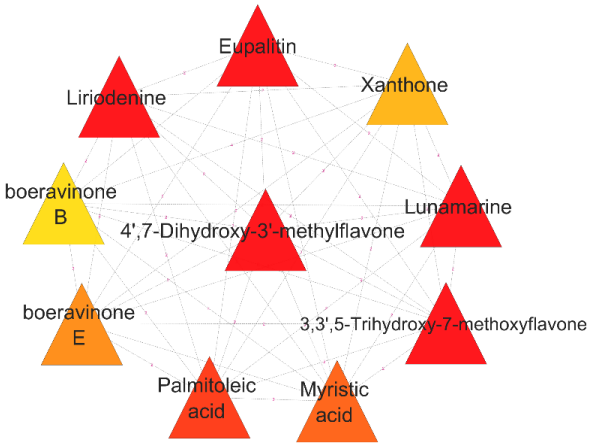

Figure 4. Sub-network representing the Hub compound.

Table 3. 2D diagrams of the Hub compounds from PubChem.

Name of compound	2D diagram
3,3′,5-trihydroxy-7-methoxyflavone	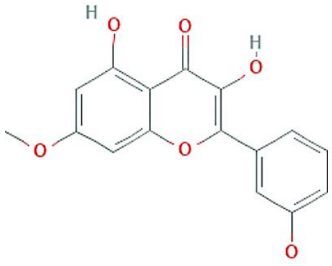
Liriodenine	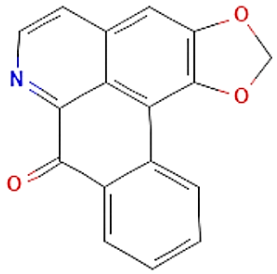
4′,7-dihydroxy-3′-methylflavone	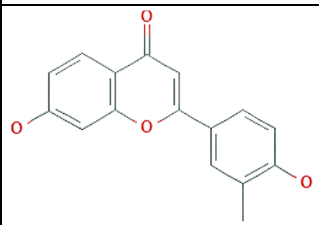
Eupalitin	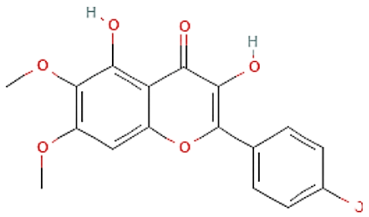
Lunamarine	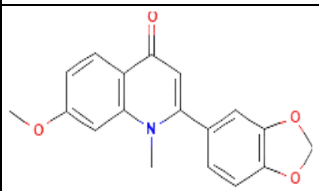

Protein-Protein Interaction Network

Figure 5 shows the PPI network resulting from importing 62 intersecting targets into the STRING database [~~53~~52]. There were 62 nodes, 912 edges, and an average node degree of 29.4 Â °. The enrichment p-value of the PPI network was less than 1.0e-16, indicating that these proteins interacted with more than a collection of randomly selected proteins would. Each node in the network reflects all proteins generated by a single gene locus that codes for the proteins. The relationships between proteins are shown at the edges. Although there may not always be a physical bond between proteins, these linkages are intended to be precise and significant, indicating that proteins work together to contribute to a common function.

The sub-network was built using the CytoHubba [~~52~~50] Plugin in Cytoscape Software [~~51~~49] to determine which Hub targets are most crucial to the growth and development of PCs. The targets were arranged according to "degree." The Hub proteins were Epidermal Growth factor (EGFR) (degree 54), RAC-alpha serine/threonine-protein kinase (AKT1) (degree 53), signal transducer and activator of transcription 3 (STAT3) (degree 50), Estrogen Receptor Alpha Gene (ESR1) (degree 49), proto-oncogene tyrosine-protein kinase Src (SRC) (degree 48), heat shock protein 90 alpha family class A member 1 (HSP90AA1) (degree 48), Erb-B2 Receptor Tyrosine Kinase 2 (ERBB2) (degree 45), transcription factor Jun (JUN) (degree 44), mouse double-minute 2 homolog (MDM2) (degree 42), and mammalian target of rapamycin (mTOR) (degree 42). Figure 6 shows the sub-network.

The colored nodes represent the query proteins and the first shell of the interactions, and the white nodes represent the second shell of interactions.  represents interactions from curated databases and  represents experimentally determined interactions. The predicted interactions in green represent the gene neighborhood, red interactions represent gene fusions, and blue interactions represent gene co-occurrence.

The rectangles represent the target proteins, and the color gradient from red to yellow represents the highest to lowest degree.

Compound-Target-Pathway (CTP) Network

The compound-target-pathway network sheds light on how the compounds in BD interact with their associated targets and how they function in different metabolic and disease-related processes. Proteoglycans in cancer, the P13K-Akt signaling pathway, the MAPK signaling pathway, and other pathways in cancer are some of the salient characteristics of this pathway. Most of the proteins targeted by BD compounds are thought to be involved in cell proliferation and tumor formation. The pathways with the highest degree of involvement were cancer, the P13K-Akt signaling pathway, MAPK signaling pathway, microRNAs in cancer, proteoglycans in cancer, Ras signaling pathway, Rap1 signaling pathway, breast cancer, gastric cancer, prostate cancer, and pancreatic cancer. Consequently, it can be said that by focusing on the aforementioned pathways, the chemicals found in BD will have protective benefits while treating cancer. Figure 7 shows a representation of the CTP network.

The relationships among the BD drugs, PC-related targets, and pathways derived from the KEGG Pathway enrichment analysis are depicted in this network. Diseases are represented by orange ellipses, chemicals by yellow rectangles, and target proteins are represented by blue ellipses. \

Molecular Docking Study

Protein Retrieval and Purification

The 3D crystal structures of the three target proteins were obtained from the RCSB PDB [~~54~~53], purified using BIOVIA Discovery Studio [~~55~~54], and structural analysis was conducted. In the structural analysis, the Ramachandran plot, secondary structure, and hydropathy plots were analyzed

(Table 4).

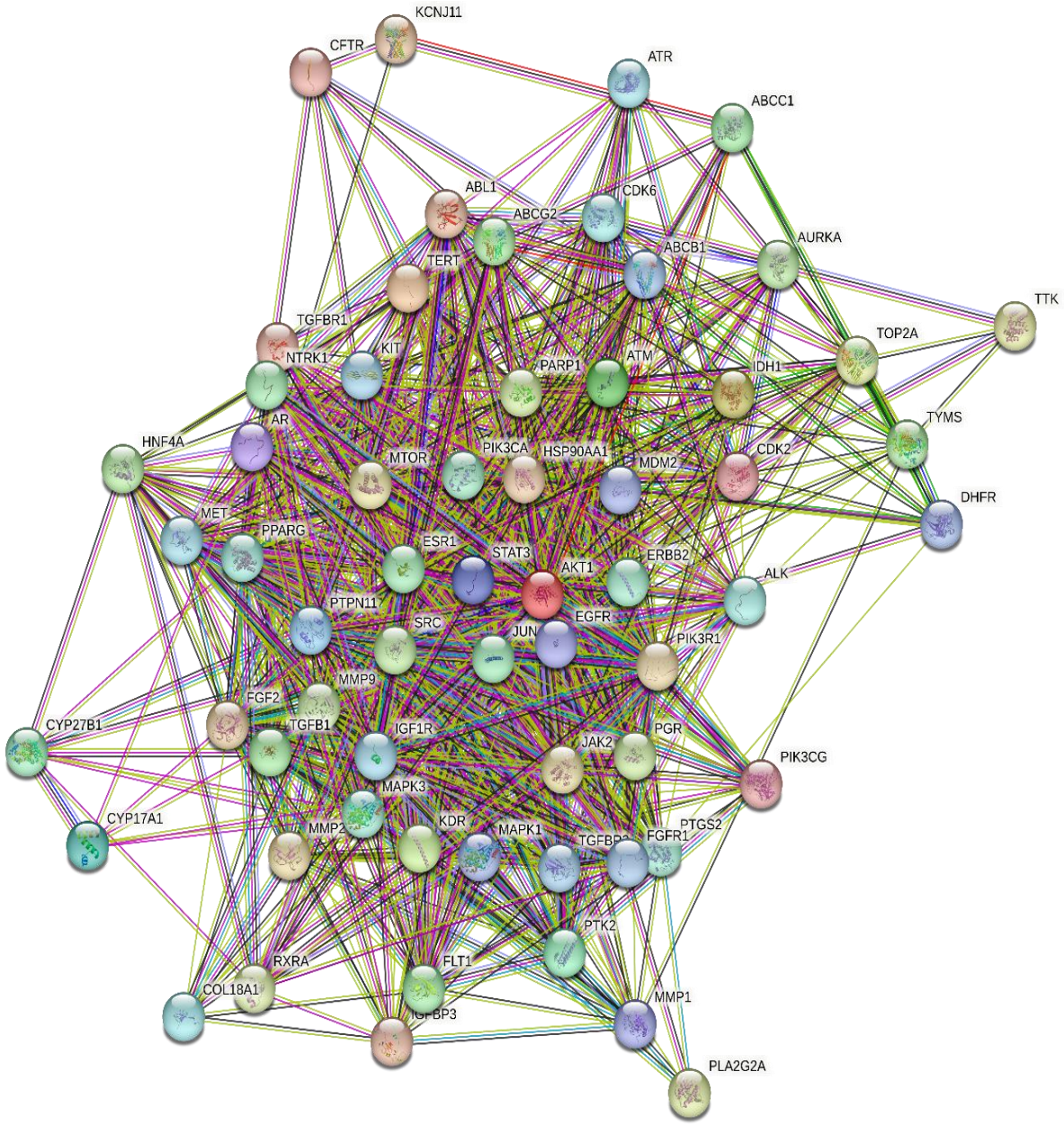

Figure 5. Protein-protein interaction network.

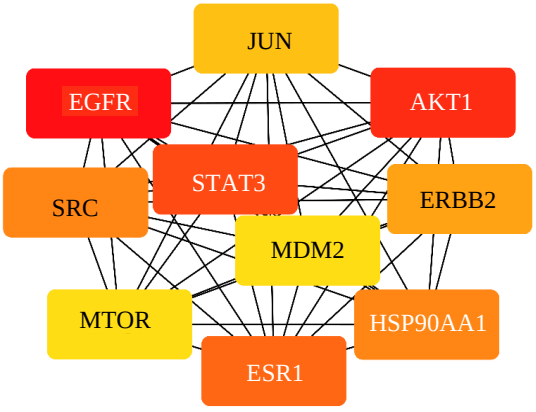

Figure 6. Sub-network representing the Hub targets.

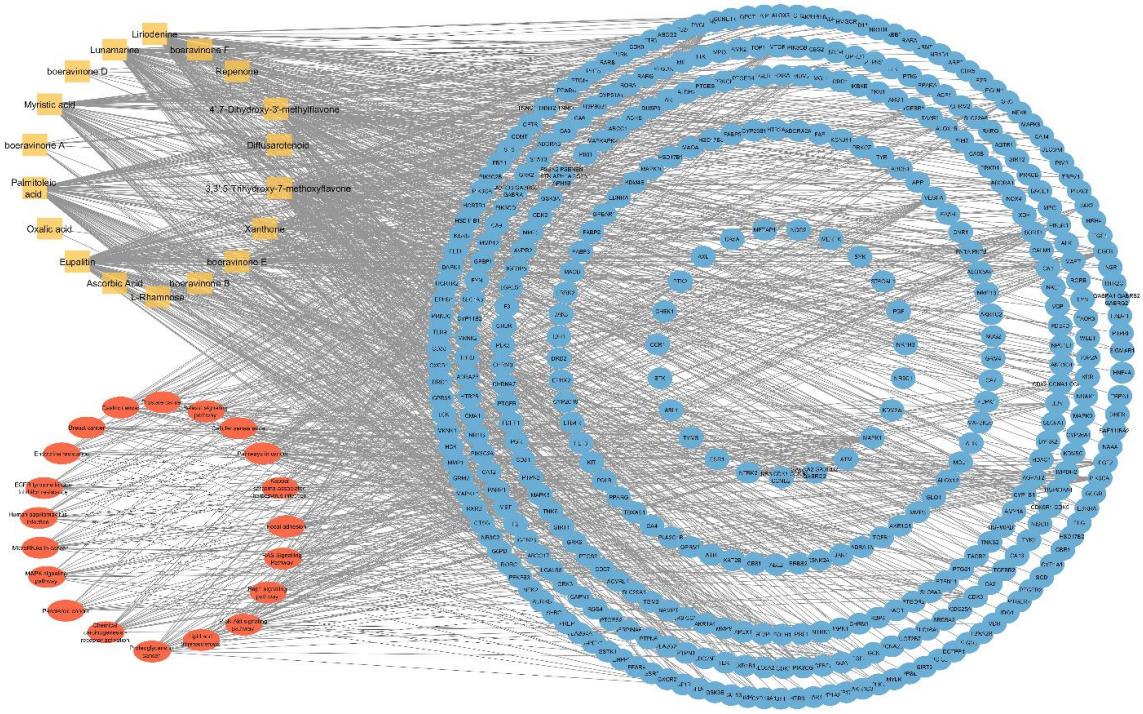

Figure 7. Compound-target-pathway network.

Table 4. Results from the structural analysis of Ramachandran Plot.

Protein	Favored region	Additional allowed regions	Generously allowed regions
EGFR	66.4%	29.1%	3.2%
AKT1	87.04%	11.7%	0.6%
STAT3	93.8%	6.2%	-

Structural Analysis Using Ramachandran Plot

Understanding Protein Conformation and Stability

Structural Analysis of Epidermal Growth Factor Receptor

The secondary structure of epidermal growth factor receptor (EGFR) is predicted to have nine sheets, two beta-alpha-beta units, five beta hairpins, four beta bulges, twenty-six strands, 13 helices, two helix-helix interactions, 77 beta turns, 12 gamma turns, and 18 disulfides, as shown in Figure 8(c). Figure 8(a) shows purified EGFR protein.

Structural Analysis of AKT1

The secondary structure of AKT1, as shown in Figure 9(c), predicts the existence of 36 beta turns, 5 gamma turns, 1 disulfide, 8 beta bulges, 7 beta hairpins, 12 strands, 15 helices, and 13 helix-helix interactions. Figure 9(a) shows purified AKT1 protein.

Structural Analysis of STAT3

Six sheets, seven beta hairpins, seven beta bulges, 20 strands, 19 helices, twenty-eight helix-helix interaction, thirty-two beta turns, and five gamma turns were predicted by the secondary structure of STAT3, as shown in Figure 10(c). Figure 10(a) shows purified STAT3 protein.

Molecular Docking

Following the sub-network analysis, three receptor proteins were chosen for molecular docking: signal transducer and activator of transcription 3 (STAT3), RAC-alpha serine/threonine-protein kinase

(AKT1), and epidermal growth factor (EGFR). The following bioactive BD compounds were selected as ligands: eupalitin, liriodenine, 4′,7-dihydroxy-3′-methylflavone, 3,3′,5-trihydroxy-7-methoxyflavone, and lunamarine. The degree of binding affinity between ligands and target proteins indicates the extent to which they bind. Table 5 shows the binding affinities of the Hub compounds to their corresponding proteins.

Molecular Docking Interaction with EGFR

Lunamarine was shown to have the greatest binding affinity (-8.1) with EGFR when the five Hub compounds were docked with EGFR. Figure 11 shows a 2D diagram of. Lunamarine binds with Cys287, Arg310, and Lys311 to form two conventional hydrogen bonds. Additionally, it creates a carbon-hydrogen connection with Ser342 and a Pi-anion link with Glu293. Asn54, Asn53, Trp80, Asp292, Ile290, Leu210, Ser205, Lys268, Leu264, Tyr272, Val270, and Val271 produced a number of van der Waals interactions.

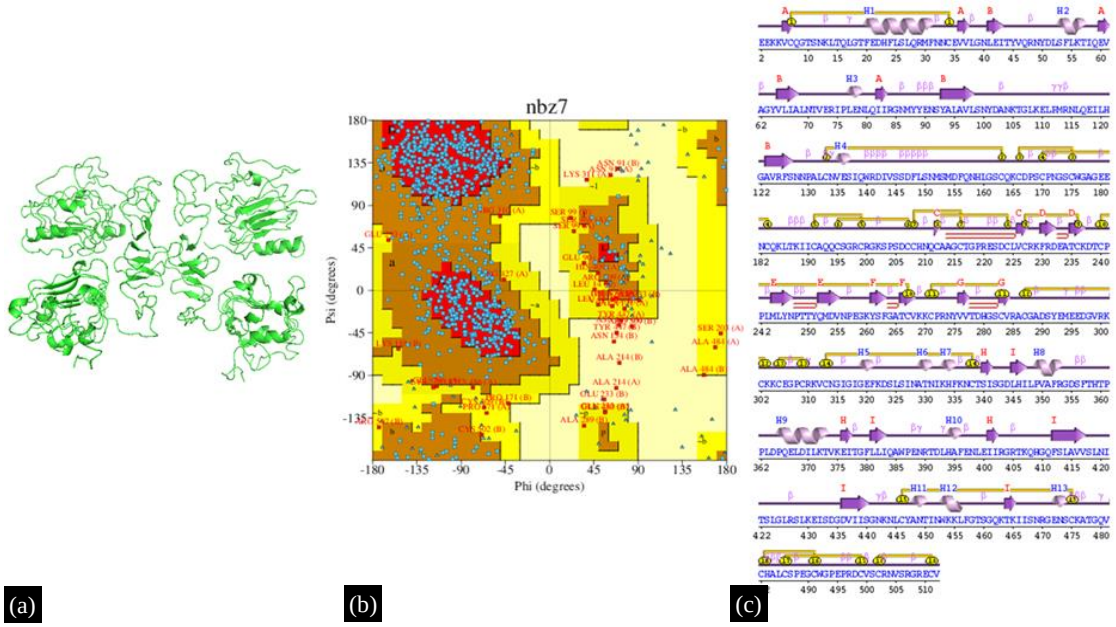

Figure 8. Structural analysis of EGFR (PDB ID: 1IVO) (a) protein EGFR'S purified protein structure, (b) Ramachandran plot, (c) predicted secondary structure.

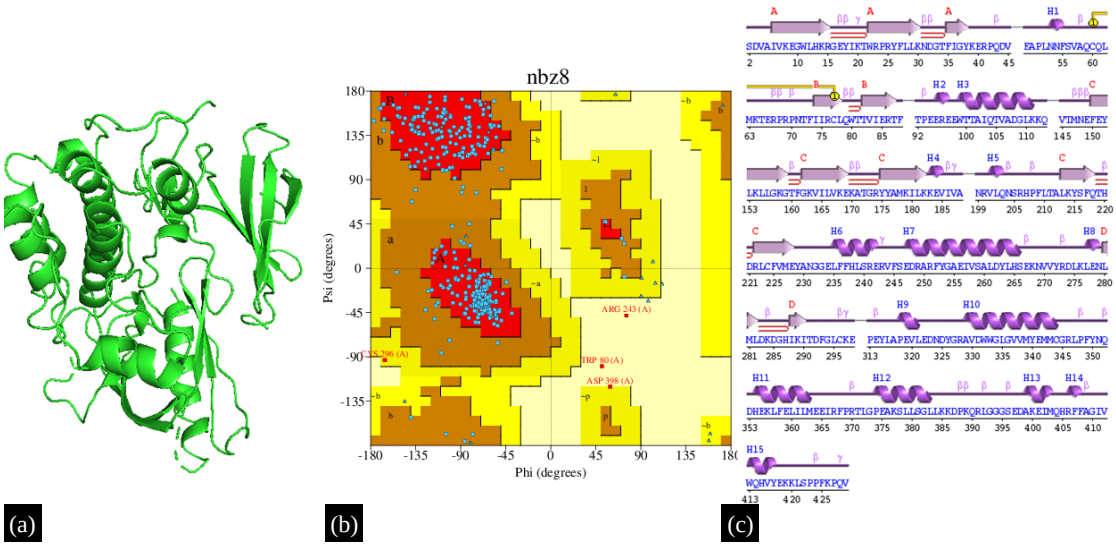

Figure 9. Structural analysis of AKT1 (PDB ID: 3O96) (a) protein AKT1 purified protein structure, (b)

Ramachandran plot, (c) predicted secondary structure.

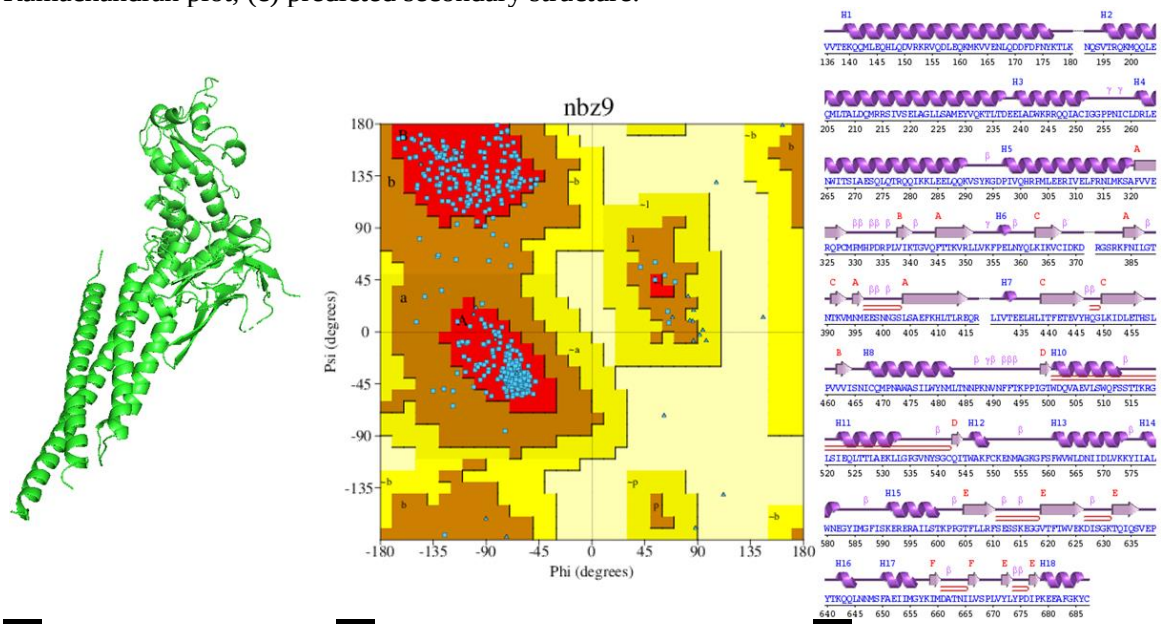

Figure 10. Structural analysis of STAT3 (PDB ID: 6NUQ) (a) protein STAT3 purified protein structure, (b) Ramachandran plot, (c) predicted secondary structure.

Table 5. Binding affinities of the ligands with their respective targets.

Compounds	**Target 1**	**Target 2**	**Target 3**
	EGFR	***AKT1***	***STAT3***
Liriodenine	-7.7	-8	-6.4
Lunamarine	-8.1	-7	-7.5
3,3′,5-trihydroxy-7-methoxyflavone	-8	-7	-7.2
4′,7-dihydroxy-3′-methylflavone	-7.8	-10	-7.8
Eupalitin	-7.9	-9	-7.1

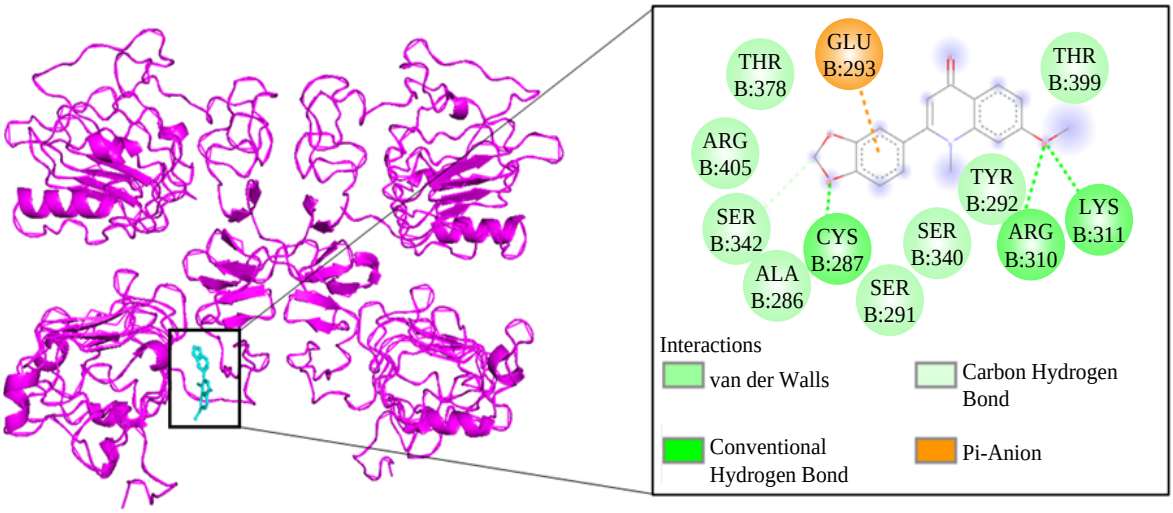

Figure 11. Represents the docked complex and the 2D visualization of EGFR and lunamarine.

Molecular Docking Interaction with AKT1

It was revealed that 4′,7-dihydroxy-3′-methylflavone exhibited the best binding affinity with AKT1

(-10), and the 2D diagram is shown in Figure 12. 4′7-dihydroxy-3′-methylflavone formed two conventional hydrogen bonds with Gln79 and Thr211, two Pi bonds with Val270 and Leu264, two Pi-Pi stacked bonds with Trp80, and two Pi-alkyl bonds with Leu210. Several van der Waals interactions were observed between Asn54, Asn53, Trp80, Asp292, Ile290, Leu210, Ser205, Lys268, Leu264, Tyr272, Val270, and Val271.

Molecular Docking Interaction with STAT3

The highest binding affinity (-7.8) was observed for the interaction between STAT3 and 4′7-dihydroxy-3′-methylflavone. Figure 13 illustrates this 2D interaction. Two Pi-Pi T-shaped bonds with Trp501, two Pi-alkyl bonds with Ala505 and Leu525, and two conventional hydrogen bonds with Ser540 and Asn538 were produced by 4′,7-dihydroxy-3′-methylflavone. Tyr539, Val537, Thr526, Ile 522, Ser509, Glu506, leu525, Asp502, and Trp501 created many van der Waals contacts.

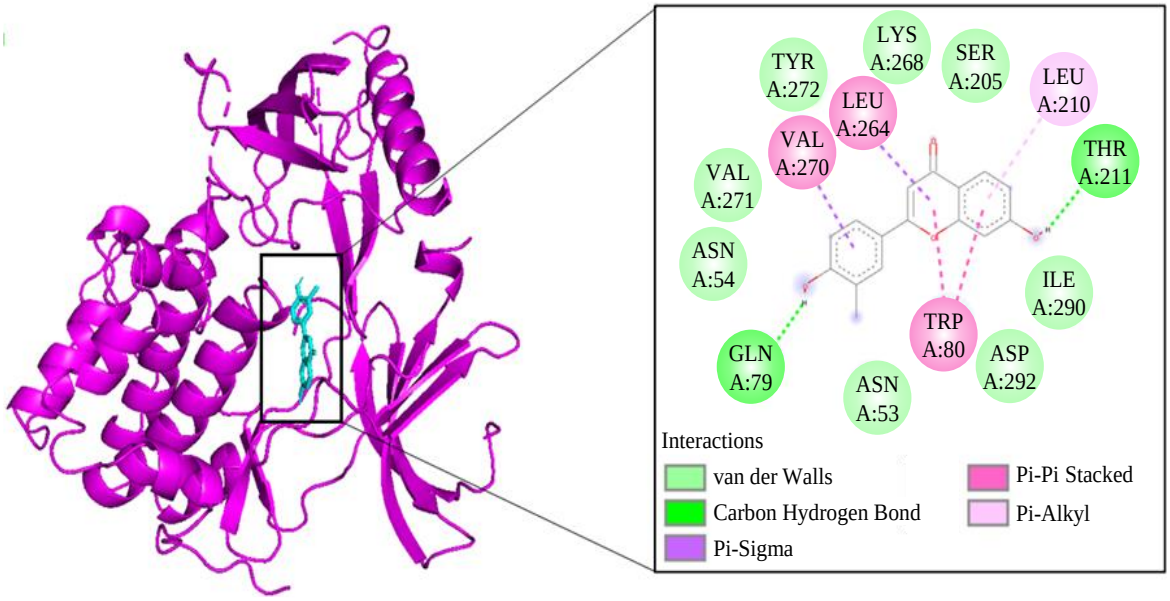

Figure 12. Represents the docked complex and the 2D visualization of AKT1 and 4′7-dihydroxy-3′-methylflavone.

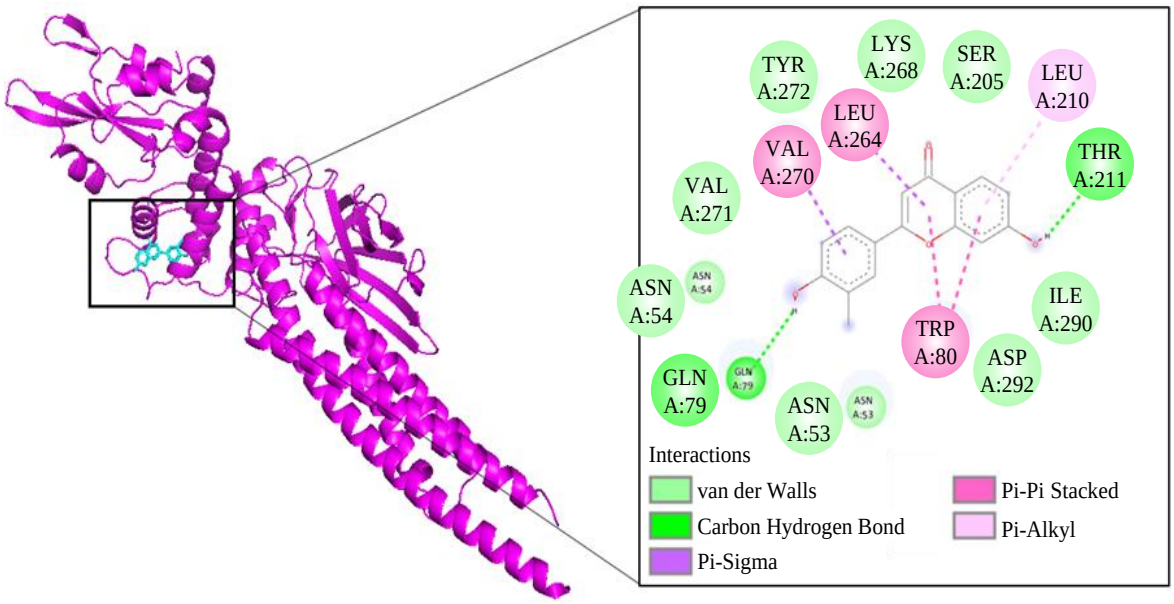

Figure 13. Represents the docked complex and the 2D visualization of STAT3 and 4′7-dihydroxy-3′-

methylflavone.

DISCUSSION

After building the CCT sub-network, the 19 compounds that passed the ADME-related metrics included 3,3′,5-trihydroxy-7-methoxyflavone, Lunamarine, 4′,7-dihydroxy-3′-methylflavone, liriodenine, and upalitin, which had the greatest degree. Lunamarine, also known as punarnavine, is a quinolone alkaloid believed to cause apoptosis by suppressing NF-kappaB-induced Bcl-2 mediated survival signaling and activating p53-induced caspase-3 mediated pro-apoptotic signaling [4955]. Ligiodenine, an isoquinoline alkaloid, ligiodenine, has been studied as a possible anti-cancer treatment, especially for ovarian cancer [5056]. It causes apoptosis by inducing caspase-3 and caspase-9, which activate the intrinsic route [5056]. The O-methylated flavanol eupalilitin has been studied in relation to prostate cancer as a possible anti-cancer drug [5149]. Eupalitin causes apoptosis by increasing the concentration of Caspase-3 and by generating ROS [5149]. It was not possible to locate pertinent data or previous research on 3,3′5-trihydroxy-7-methoxyflavone and 4′7-dihydroxy-3′-methylflavone.

The most frequently engaged protein in PC, according to a deeper examination of the PPI network sub-network based on degree, is the EGFR. The ErbB family of receptor tyrosine kinases (RTKs) include the EGFR protein, which is involved in many aspects of epithelial cell physiology. It has been shown that PC is frequently associated with overexpression of both epidermal growth factor (EGF) and EGFR [5250]. As it is commonly mutated and/or overexpressed in several human cancer types, it is a target for multiple cancer therapies [5352]. The primary ligands of EGFR are TGF-β and EGF, and EGFR mutations typically occur in the form of overexpression, mutation, deletion, and rearrangement. These alterations cause tyrosine kinases to become active, which can aid in the onset and spread of PC [5453]. Cell proliferation is thought to result from the binding of EGF to epidermal growth factor receptor (EGFR), which in turn causes homodimerization or heterodimerization with ErbB receptors such as HER2, receptor phosphorylation, and activation of downstream effectors such as RAS-RAF-MEK-ERK-MAPK and PI3K-AKT-mTOR [5554]. When tyrosine residues are transphosphorylated intracellularly owing to dimerization, several cell signaling pathways are activated, including P13K, Src, MAPK, and signal transducer and activator of transcription (STAT) [5453]. This stimulates cell division, cell cycle progression, invasion, and metastasis. Given that advanced clinical stages of PC have been associated with greater EGFR expression, deregulation of the EGFR pathway has also been linked to poor prognoses for patients with PC [5453]. Approximately 90% of PDAC patients have the G12 mutation in KRAS, making KRAS one of the most frequently found mutations in human solid tumors [5657–5960]. Lunamarine was the Hub compound with the highest binding affinity (-8.1) when EGFR was docked with it. Partial binding took place in the sixth and seventh active sites when the residues involved in binding were compared with the residues of the active sites. Therefore, lunamarine possesses characteristics that would make it a potent EGFR inhibitor.

The protein known as serine/threonine-protein kinases-1 (AKT1) had the second-highest degree within the PPI network sub-network. Protein Kinase B (AKT) kinases are important intermediaries in pathways governing cell growth, proliferation, survival, glucose metabolism, genomic stability, and neovascularization [6061]. In vivo studies using genetically engineered mice have shown that aberrant AKT signaling, either on its own or in conjunction with other genetic changes, contributes to cancer [6162, 6263]. AKT is involved in multiple signaling pathways that include elements linked to tumorigenesis, including downstream tuberous sclerosis complex 2 (TSC2), Forkhead Box Class O (FOXO), eukaryotic initiation factor 4E (eIF4E), upstream phosphatidylinositol 3-kinase (PI3K), Phosphatase and Tensin homolog deleted on chromosome Ten), NF1, and LKB1. Additionally, AKT activates IκB kinase, which causes the transcription of anti-apoptotic proteins and favorably regulates NF-κB [6364]. AKT also facilitates the phosphorylation and translocation of mdm2 into the nucleus, which downregulates p53 and obstructs p53-mediated cell cycle checkpoints [6465, 6566]. Therefore, it may be possible to treat PC by blocking AKT1, which is thought to be essential for the PI3K-AKT-mTOR pathway. The highest binding affinity was observed for 4′,7-dihydroxy-3′-methylflavone when the 5-Hub compounds were docked with AKT1 (-10). The results from PrankWeb [4848] indicated that

binding occurs at the first active site. Given that 4′,7-dihydroxy-3′-methylflavone interacts with the first active site and has a high binding affinity, it is worth investigating as a possible AKT1 inhibitor. The STAT family, which includes STAT1, TAT2, STAT3, STAT4, STAT5A, STAT5B, and STAT6, is involved in the control of cytokine-dependent inflammation and immunity [~~66~~67]. Studies have been conducted on the role of STAT3 in inflammation and cancer. Numerous studies have revealed that IL-6/JAK2/STAT3 is highly activated in PC and associated with the occurrence, development, metastasis, and invasion of tumors, in addition to being involved in a number of physiological and pathological processes such as angiogenesis, cell proliferation, immune regulation, and differentiation [~~67~~68, ~~68~~69]. Cytokines participating in the gp130 or homodimeric cytokine receptor chain, as well as some growth factors operating via protein tyrosine kinase receptors, activate STAT3 [~~69~~70– ~~71~~72]. Therefore, STAT3 is involved in intracellular signal transduction and tumorigenic signaling pathways, including the NF-κB pathway [~~72~~73], G-CSF-STAT3 route [~~73~~74], and IL-11-STAT3 signaling [~~74~~75]. Through direct tumor autonomic mechanisms or indirect regulation of the immune system and stroma relevant to the tumor's anti-tumor responses, STAT3 can encourage the development of tumors [~~74~~75]. The optimal binding affinity was found for 4′,7-dihydroxy-3′-methylflavone following STAT3 molecular docking with the Hub compounds (-7.8). It was discovered that the binding takes place at the eighth active site when these residues were compared to those of the active sites. Thus, 4′,7-dihydroxy-3′-methylflavone may be investigated further as a possible STAT3 inhibitor.

GO and KEGG Pathway Enrichment analyses suggested that the nucleus, cytoplasm, plasma membrane, cytosol, nucleoplasm, and receptor complex were among the most enriched cellular components. Protein-binding, DNA-binding, and protein serine/threonine/kinase activities were the most abundant. These activities are essential for controlling cell growth, survival, and cycle progression [~~75~~76], and any abnormal expression can result in the development and spread of tumors. Therefore, blocking protein targets implicated in these pathways and processes can effectively cure PC.

CONCLUSIONS

This study employed a network pharmacology method to examine the molecular processes of *Boerhavia diffusa* in the context of pancreatic cancer therapy. According to our study, 4′,7-dihydroxy-3′-methylflavone and lunamarine have anti-pancreatic cancer effects. Moreover, it has been shown that STAT3, AKT1, and EGFR have been shown to have major impacts on pancreatic cancer. Recent findings are anticipated to help researchers conduct further studies to validate the essential compounds o*f Boerhavia diffusa* against pancreatic cancer for possible therapeutic applications. However, this study had several limitations. For example, although the anti-tumor and immunomodulatory properties of the substances under analysis have been the subject of several clinical trials, further validation is required. Furthermore, it is crucial to confirm the scientific validity and rationale of the predicted targets through in vitro and in vivo studies.

Acknowledgments

I would like to thank BioNome for offering support with scientific research services.

REFERENCES

1. Parkin DM, Bray F, Ferlay J, Pisani P. Global cancer statistics, 2002. CA Cancer J Clin. 2005;55:74-108. DOI: 10.3322/canjclin.55.2.74, PubMed: 15761078.
2. Gillen S, Schuster T, Meyer Zum Büschenfelde C, Friess H, Kleeff J. Preoperative/neoadjuvant therapy in pancreatic cancer: A systematic review and meta-analysis of response and resection percentages. PLoS Med. 2010;7. DOI: 10.1371/journal.pmed.1000267, PubMed: 20422030.
3. Kamisawa T, Wood LD, Itoi T, Takaori K. Pancreatic cancer. Lancet. 2016;388:73-85. DOI: 10.1016/S0140-6736(16)00141-0, PubMed: 26830752.
4. He J, Page AJ, Weiss M, Wolfgang CL, Herman JM, Pawlik TM. Management of borderline and locally advanced pancreatic cancer: Where do we stand? World J Gastroenterol. 2014;20:2255-66. DOI: 10.3748/wjg.v20.i9.2255, PubMed: 24605025.
5. Seufferlein T, Hammel P, Delpero JR, et al. Optimizing the management of locally advanced

pancreatic cancer with a focus on induction chemotherapy: Expert opinion based on a review of current evidence. Cancer Treat Rev. 2019;77:1-10. DOI: 10.1016/j.ctrv.2019.05.007, PubMed: 31163334.
6. Loehrer PJ Sr, Feng Y, Cardenes H, et al. Gemcitabine alone versus gemcitabine plus radiotherapy in patients with locally advanced pancreatic cancer: An Eastern Cooperative Oncology Group trial. J Clin Oncol. 2011;29:4105-12. DOI: 10.1200/JCO.2011.34.8904, PubMed: 21969502.
7. Zhen DB, Coveler A, Zanon S, Reni M, Chiorean EG. Biomarker-driven and molecularly targeted therapies for pancreatic adenocarcinoma. Semin Oncol. 2018;45:107-15. DOI: 10.1053/j.seminoncol.2018.05.004, PubMed: 30391013.
8. Mizrahi JD, Surana R, Valle JW, Shroff RT. Pancreatic cancer. The Lancet. 2020 Jun 27;395(10242):2008-20.
9. Sherman MH, Beatty GL. Tumor microenvironment in pancreatic cancer pathogenesis and therapeutic resistance. Annu Rev Pathol. 2023;18:123-48. DOI: 10.1146/annurev-pathmechdis-031621-024600. Epub 2022 Sep 21. PubMed: 36130070, PubMed Central: PMC9877114.
10. Beatty GL, Werba G, Lyssiotis CA, Simeone DM. The biological underpinnings of therapeutic resistance in pancreatic cancer. Genes Dev. 2021;35:940-62. DOI: 10.1101/gad.348523.121, PubMed: 34117095.
11. Siegel RL, Miller KD, Fuchs HE, Jemal A. Cancer statistics, 2022. CA Cancer J Clin. 2022;72:7-33. DOI: 10.3322/caac.21708, PubMed: 35020204.
12. Conklin KA. Chemotherapy-associated oxidative stress: Impact on chemotherapeutic effectiveness. Integr Cancer Ther. 2004;3:294-300. DOI: 10.1177/1534735404270335, PubMed: 15523100.
13. Jaiswal YS, Williams LL. A glimpse of Ayurveda – The forgotten history and principles of Indian traditional medicine. J Tradit Complement Med. 2017;7:50-3. DOI: 10.1016/j.jtcme.2016.02.002, PubMed: 28053888.
14. Dutta R, Khalil R, Green R, Mohapatra SS, Mohapatra S. Withania somnifera (Ashwagandha) and Withaferin A: Potential in integrative oncology. Int J Mol Sci. 2019;20:5310. DOI: 10.3390/ijms20215310, PubMed: 31731424.
15. Shimizu T, Torres MP, Chakraborty S, et al. Holy Basil leaf extract decreases tumorigenicity and metastasis of aggressive human pancreatic cancer cells in vitro and in vivo: Potential role in therapy. Cancer Lett. 2013;336:270-80. DOI: 10.1016/j.canlet.2013.03.017, PubMed: 23523869.
16. Akimoto M, Iizuka M, Kanematsu R, Yoshida M, Takenaga K. Anticancer effect of ginger extract against pancreatic cancer cells mainly through reactive oxygen species-mediated autotic cell death. PLoS One. 2015;10. DOI: 10.1371/journal.pone.0126605, PubMed: 25961833.
17. Rao SK, Rao PS, Rao BN. Preliminary investigation of the radiosensitizing activity of guduchi (Tinospora cordifolia) in tumor-bearing mice. Phytother Res. 2008;22:1482-9. DOI: 10.1002/ptr.2508, PubMed: 18803246.
18. Poornima P, Efferth T. Ayurveda for cancer treatment. Med Aromat Plants. 2016;5:5. DOI: 10.4172/2167-0412.1000e178.
19. Govindarajan R, Vijayakumar M, Pushpangadan P. Antioxidant approach to disease management and the role of 'Rasayana' herbs of Ayurveda. J Ethnopharmacol. 2005;99:165-78. DOI: 10.1016/j.jep.2005.02.035, PubMed: 15894123.
20. Bairwa K, Srivastava A, Jachak SM. Quantitative analysis of boeravinones in the roots of Boerhaavia diffusa by UPLC/PDA. Phytochem Anal. 2014;25:415-20. DOI: 10.1002/pca.2509, PubMed: 24677242.
21. Srivastava R, Saluja D, Chopra M. Isolation and screening of anticancer metabolites from Boerhavia diffusa. Indian J Med Res. 2005;151(Suppl 1).
22. Mungantiwar AA, Nair AM, Kamal KK, Saraf MN. Adaptogenic activity of aqueous extract of the roots of Boerhaavia diffusa Linn. Indian Drugs. 1997;34:184-9.
23. Karole S, Shrivastava S, Thomas S, et al. Polyherbal formulation concept for synergic action: A review. J Drug Deliv Ther. 2019;9:453-66. DOI: 10.22270/jddt.v9i1-s.2339.
24. Hopkins AL. Network pharmacology. Nat Biotechnol. 2007;25(10):1110–1. DOI:

10.1038/nbt1007-1110, PubMed: 17921993.
25. Zhang B, Wang X, Li S. An integrative platform of TCM network pharmacology and its application on a herbal formula, Qing-Luo-Yin. Evid Based Complement Alternat Med. 2013;2013:456747. DOI: 10.1155/2013/456747, PubMed: 23653662.
26. Berger SI, Iyengar R. Network analyses in systems pharmacology. Bioinformatics. 2009;25(19):2466–72. DOI: 10.1093/bioinformatics/btp465, PubMed: 19648136.
27. Kibble M, Saarinen N, Tang J, Wennerberg K, Mäkelä S, Aittokallio T. Network pharmacology applications to map the unexplored target space and therapeutic potential of natural products. Nat Prod Rep. 2015;32(9):1249–66. DOI: 10.1039/c5np00005j, PubMed: 26030402.
28. Liu X, Zhou H. Application of proteomics technique in study of network pharmacology. Prog Pharm Sci. 2014;38:89–96.
29. Mohanraj K, Karthikeyan BS, Vivek-Ananth RP, Chand RPB, Aparna SR, Mangalapandi P, Samal A. IMPPAT: A curated database of Indian medicinal plants, phytochemistry and therapeutics. Sci Rep. 2018;8:4329. DOI: 10.1038/s41598-018-22631-z, PubMed: 29531263.
30. Barton HA, Pastoor TP, Baetcke K, Chambers JE, Diliberto J, Doerrer NG, et al. The acquisition and application of absorption, distribution, metabolism, and excretion (ADME) data in agricultural chemical safety assessments. Crit Rev Toxicol. 2006;36(1):9–35. DOI: 10.1080/10408440500534362, PubMed: 16708693.
31. Daina A, Michielin O, Zoete V. SwissADME: A free web tool to evaluate pharmacokinetics, drug-likeness and medicinal chemistry friendliness of small molecules. Sci Rep. 2017;7:42717. DOI: 10.1038/srep42717, PubMed: 28256516.
32. Xiong G, Wu Z, Yi J, Fu L, Yang Z, Hsieh C, et al. ADMETlab 2.0: An integrated online platform for accurate and comprehensive predictions of ADMET properties. Nucleic Acids Res. 2021;49–W14. DOI: 10.1093/nar/gkab255, PubMed: 33893803, PubMed Central: PMC8262709.
33. Gfeller D, Grosdidier A, Wirth M, Daina A, Michielin O, Zoete V. SwissTargetPrediction: A web server for target prediction of bioactive small molecules. Nucleic Acids Res. 2014;42(Web Server issue)W32–8. DOI: 10.1093/nar/gku293, PubMed: 24792161, PubMed Central: PMC4086140.
34. Keiser MJ, Roth BL, Armbruster BN, Ernsberger P, Irwin JJ, Shoichet BK. Relating protein pharmacology by ligand chemistry. Nat Biotechnol. 2007;25(2):197–206. DOI: 10.1038/nbt1284, PubMed: 17287757.
35. Stelzer G, Rosen N, Plaschkes I, Zimmerman S, Twik M, Fishilevich S, et al. The GeneCards suite: From gene data mining to disease genome sequence analyses. Curr Protoc Bioinformatics. 2016;54:1.30.1–33. DOI: 10.1002/cpbi.5, PubMed: 27322403.
36. Oliveros JC. Venny. An interactive tool for comparing lists with Venn's diagrams. 2007–15. Available from: https://bioinfogp.cnb.csic.es/tools/venny/index.html.
37. Dennis G, Sherman BT, Hosack DA, Yang J, Gao W, Lane HC, Lempicki RA. DAVID: Database for Annotation, Visualization, and Integrated Discovery. Genome Biol. 2003;4(5). DOI: 10.1186/gb-2003-4-9-r60, PubMed: 12734009.
38. Tang D, Chen M, Huang X, Zhang G, Zeng L, Zhang G, et al. SRplot: A free online platform for data visualization and graphing. PLoS One. 2023;18. DOI: 10.1371/journal.pone.0294236, PubMed: 37943830.
39. Shannon P, Markiel A, Ozier O, Baliga NS, Wang JT, Ramage D, et al. Cytoscape: A software environment for integrated models of biomolecular interaction networks. Genome Res. 2003;13(11):2498–504. DOI: 10.1101/gr.1239303, PubMed: 14597658, PubMed Central: PMC403769.
40. Chin CH, Chen SH, Wu HH, Ho CW, Ko MT, Lin CY. cytoHubba: Identifying hub objects and sub-networks from complex interactome. BMC Syst Biol. 2014;8(Suppl 4). DOI: 10.1186/1752-0509-8-S4-S11, PubMed: 25521941, PubMed Central: PMC4290687.
41. Szklarczyk D, Gable AL, Lyon D, Junge A, Wyder S, Huerta-Cepas J, et al. STRING v11: Protein–protein association networks with increased coverage, supporting functional discovery in genome-wide experimental datasets. Nucleic Acids Res. 2019;47–13. DOI: 10.1093/nar/gky1131, PubMed:

30476243, PubMed Central: PMC6323986.
42. RCSB Protein Data Bank A resource for chemical, biochemical, and structural explorations of large and small biomolecules. Christine Zardecki, Shuchismita Dutta, David S. Goodsell, Maria Voigt, and Stephen K. Burley.
43. BIOVIA, Dassault Systèmes, Discovery Studio visualizer, version 21.1.0 Dassault systèmes: San Diego; 2021.
44. Pettersen EF, Goddard TD, Huang CC, Couch GS, Greenblatt DM, Meng EC, Ferrin TE. UCSF Chimera—A visualization system for exploratory research and analysis. J Comput Chem. 2004;25(13):1605–12. DOI: 10.1002/jcc.20084, PubMed: 15264254.
45. Laskowski RA, Jabłońska J, Pravda L, Vařeková RS, Thornton JM. PDBsum: Structural summaries of PDB entries. Protein Sci. 2018;27:129–34. doi: 10.1002/pro.3289. Epub 2017 Oct 27. PubMed: 28875543; PubMed Central: PMC5734310.
46. Dallakyan S, Olson AJ. Small-molecule library screening by docking with PyRx. Methods Mol Biol. 2015;1263:243–50. doi: 10.1007/978-1-4939-2269-7_19. PubMed: 25618350.
47. PhysiologyMOL molecular graphics system, version 1.2r. Schrödinger, LLC: Portland, USA.
48. Jendele L, Krivak R, Skoda P, Novotny M, Hoksza D. PrankWeb: A web server for ligand binding site prediction and visualization. Nucleic Acids Res. 2019;47–9. doi: 10.1093/nar/gkz424. PubMed: 31114880; PubMed Central: PMC6602436.
49. Kaleem S, Siddiqui S, Siddiqui HH, Badruddeen HA, Hussain A, Arshad M, et al. Eupalitin induces apoptosis in prostate carcinoma cells through ROS generation and increase of caspase-3 activity. Cell Biol Int. 2016;40:196–203. doi: 10.1002/cbin.10552. PubMed: 26493029.
50. Schlessinger J. Receptor tyrosine kinases: Legacy of the first two decades. Cold Spring Harb Perspect Biol. 2014;6. doi: 10.1101/cshperspect.a008912. PubMed: 24591517.
51. Kim S, Chen J, Cheng T, Gindulyte A, He J, He S, et al. PubChem 2023 update. Nucleic Acids Res. 2023;51–80. doi: 10.1093/nar/gkac956. PubMed: 36305812.
52. Yarden Y, Pines G. The ERBB network: At last, cancer therapy meets systems biology. Nat Rev Cancer. 2012;12:553–63. doi: 10.1038/nrc3309. PubMed: 22785351.
53. Sarkar FH, Banerjee S, Li Y. Pancreatic cancer: Pathogenesis, prevention and treatment. Toxicol Appl Pharmacol. 2007;224:326–36. doi: 10.1016/j.taap.2006.11.007. Epub 2006 Nov 11. PubMed: 17174370; PubMed Central: PMC2094388.
54. Ciardiello F, Tortora G. EGFR antagonists in cancer treatment. N Engl J Med. 2008;358:1160–74. doi: 10.1056/NEJMra0707704. PubMed: 18337605.
~~48.~~
~~49.~~55. Manu KA, Kuttan G. Punarnavine induces apoptosis in B16F-10 melanoma cells by inhibiting NF-kappaB signaling. Asian Pac J Cancer Prev. 2009;10:1031–7. PubMed: 20192578.
~~50.~~56. Nordin N, Majid NA, Hashim NM, Rahman MA, Hassan Z, Ali HM. Liriodenine, an aporphine alkaloid from Enicosanthellum pulchrum, inhibits proliferation of human ovarian cancer cells through induction of apoptosis via the mitochondrial signaling pathway and blocking cell cycle progression. Drug Des Dev Ther. 2015;9:1437–48. doi: 10.2147/DDDT.S77727. PubMed: 25792804; PubMed Central: PMC4362660.
~~51.~~1. ~~Kaleem S, Siddiqui S, Siddiqui HH, Badruddeen HA, Hussain A, Arshad M, et al. Eupalitin induces apoptosis in prostate carcinoma cells through ROS generation and increase of caspase-3 activity. Cell Biol Int. 2016;40:196–203. doi: 10.1002/cbin.10552. PubMed: 26493029.~~
~~52.~~1. ~~Schlessinger J. Receptor tyrosine kinases: Legacy of the first two decades. Cold Spring Harb Perspect Biol. 2014;6. doi: 10.1101/cshperspect.a008912. PubMed: 24591517.~~
~~53.~~1. ~~Yarden Y, Pines G. The ERBB network: At last, cancer therapy meets systems biology. Nat Rev Cancer. 2012;12:553–63. doi: 10.1038/nrc3309. PubMed: 22785351.~~
~~54.~~1. ~~Sarkar FH, Banerjee S, Li Y. Pancreatic cancer: Pathogenesis, prevention and treatment. Toxicol Appl Pharmacol. 2007;224:326–36. doi: 10.1016/j.taap.2006.11.007. Epub 2006 Nov 11. PubMed: 17174370; PubMed Central: PMC2094388.~~
~~55.~~1. ~~Ciardiello F, Tortora G. EGFR antagonists in cancer treatment. N Engl J Med. 2008;358:1160–74. doi: 10.1056/NEJMra0707704. PubMed: 18337605.~~

~~56.~~57. Knudsen ES, O'Reilly EM, Brody JR, Witkiewicz AK. Genetic diversity of pancreatic ductal adenocarcinoma and opportunities for precision medicine. Gastroenterology. 2016;150:48–63. doi: 10.1053/j.gastro.2015.08.056. PubMed: 26385075.

~~57.~~58. Kanda M, Matthaei H, Wu J, Hong SM, Yu J, Borges M, et al. Presence of somatic mutations in most early-stage pancreatic intraepithelial neoplasia. Gastroenterology. 2012;142:730–3.e9. doi: 10.1053/j.gastro.2011.12.042. PubMed: 22226782.

~~58.~~59. Cox AD, Fesik SW, Kimmelman AC, Luo J, Der CJ. Drugging the undruggable RAS: Mission possible? Nat Rev Drug Discov. 2014;13:828–51. doi: 10.1038/nrd4389. PubMed: 25323927.

~~59.~~60. Qian ZR, Rubinson DA, Nowak JA, Morales-Oyarvide V, Dunne RF, Kozak MM, et al. Association of alterations in main driver genes with outcomes of patients with resected pancreatic ductal adenocarcinoma. JAMA Oncol. 2018;4. doi: 10.1001/jamaoncol.2017.3420. PubMed: 29098284.

~~60.~~61. Bellacosa A, Kumar CC, Di Cristofano A, Testa JR. Activation of AKT kinases in cancer: Implications for therapeutic targeting. Adv Cancer Res. 2005;94:29–86. doi: 10.1016/S0065-230X(05)94002-5. PubMed: 16095999.

~~61.~~62. Luo J, Manning BD, Cantley LC. Targeting the PI3K-Akt pathway in human cancer: Rationale and promise. Cancer Cell. 2003;4:257–62. doi: 10.1016/s1535-6108(03)00248-4. PubMed: 14585353.

~~62.~~63. Bjornsti MA, Houghton PJ. Lost in translation: Dysregulation of cap-dependent translation and cancer. Cancer Cell. 2004;5:519–23. doi: 10.1016/j.ccr.2004.05.027. PubMed: 15193254.

~~63.~~64. Pommier Y, Sordet O, Antony S, Hayward RL, Kohn KW. Apoptosis defects and chemotherapy resistance: Molecular interaction maps and networks. Oncogene. 2004;23:2934–49. doi: 10.1038/sj.onc.1207515. PubMed: 15077155.

~~64.~~65. Mayo LD, Donner DB. The PTEN, Mdm2, p53 tumor suppressor-oncoprotein network. Trends Biochem Sci. 2002;27:462–7. doi: 10.1016/s0968-0004(02)02166-7. PubMed: 12217521.

~~65.~~66. Zhou BP, Hung MC. Novel targets of Akt, p21(Cipl/WAF1), and MDM2. Semin Oncol. 2002;29(Suppl 11):62–70. doi: 10.1053/sonc.2002.34057. PubMed: 12138399.

~~66.~~67. Fang X, Hong Y, Dai L, Qian Y, Zhu C, Wu B, et al. CRH promotes human colon cancer cell proliferation via IL-6/JAK2/STAT3 signaling pathway and VEGF-induced tumor angiogenesis. Mol Carcinog. 2017;56:2434–45. doi: 10.1002/mc.22691. PubMed: 28618089.

~~67.~~68. Zhang X, Lu H, Hong W, Liu L, Wang S, Zhou M, et al. Tyrphostin B42 attenuates trichostatin A-mediated resistance in pancreatic cancer cells by antagonizing IL-6/JAK2/STAT3 signaling. Oncol Rep. 2018;39:1892–900. doi: 10.3892/or.2018.6241. PubMed: 29393444.

~~68.~~69. Fresno Vara JA, Casado E, de Castro J, Cejas P, Belda-Iniesta C, González-Barón M. PI3K/Akt signalling pathway and cancer. Cancer Treat Rev. 2004;30:193–204. doi: 10.1016/j.ctrv.2003.07.007. PubMed: 15023437.

~~69.~~70. Hillmer EJ, Zhang H, Li HS, Watowich SS. STAT3 signaling in immunity. Cytokine Growth Factor Rev. 2016;31:1–15. doi: 10.1016/j.cytogfr.2016.05.001. PubMed: 27185365.

~~70.~~71. Zhong Z, Wen Z, Darnell JE Jr. Stat3: A STAT family member activated by tyrosine phosphorylation in response to epidermal growth factor and interleukin-6. Science. 1994;264:95–8. doi: 10.1126/science.8140422. PubMed: 8140422.

~~71.~~72. Ruff-Jamison S, Zhong Z, Wen Z, Chen K, Darnell JE Jr, Cohen S. Epidermal growth factor and lipopolysaccharide activate Stat3 transcription factor in mouse liver. J Biol Chem. 1994;269:21933–5. doi: 10.1016/S0021-9258(17)31735-0. PubMed: 8071311.

~~72.~~73. Wang D, Zheng X, Fu B, Nian Z, Qian Y, Sun R, et al. Hepatectomy promotes recurrence of liver cancer by enhancing IL-11-STAT3 signaling. EBiomedicine. 2019;46:119–32. doi: 10.1016/j.ebiom.2019.07.058. PubMed: 31375423.

~~73.~~74. Nguyen-Jackson HT, Li HS, Zhang H, Ohashi E, Watowich SS. G-CSF-activated STAT3 enhances production of the chemokine MIP-2 in bone marrow neutrophils. J Leukoc Biol. 2012;92:1215–25. doi: 10.1189/jlb.0312126. PubMed: 23024284.

~~74.~~75. Taniguchi K, Karin M. NF-κB, inflammation, immunity and cancer: Coming of age. Nat Rev Immunol. 2018;18:309–24. doi: 10.1038/nri.2017.142. PubMed: 29379212.

~~75.~~76. Fresno Vara JA, Casado E, de Castro J, Cejas P, Belda-Iniesta C, González-Barón M. PI3K/Akt signalling pathway and cancer. Cancer Treat Rev. 2004 Apr;30(2):193-204. doi: 10.1016/j.ctrv.2003.07.007. PMID: 15023437.

~~76.1. Kim S, Chen J, Cheng T, Gindulyte A, He J, He S, et al. PubChem 2023 update. Nucleic Acids Res. 2023;51–80. doi: 10.1093/nar/gkac956. PubMed: 36305812.~~

